Defects in virgin and N⁺-implanted ZnO single crystals studied by positron annihilation, Hall effect, and deep-level transient spectroscopy

G. Brauer,[*] W. Anwand, and W. Skorupa

Institut für Ionenstrahlphysik und Materialforschung, Forschungszentrum Rossendorf, Postfach 510119, D-01314 Dresden, Germany

J. Kuriplach[†] and O. Melikhova

Department of Low Temperature Physics, Faculty of Mathematics and Physics, Charles University, V Holešovičkách 2, CZ-18000 Prague 8, Czech Republic

C. Moisson[‡]

NOVASiC, Savoie Technolac-Arche Bât. 4, Boîte Postal 267, F-73375 Le Bourget du Lac Cedex, France

H. von Wenckstern,[§] H. Schmidt, M. Lorenz, and M. Grundmann

Institut für Experimentelle Physik II, Universität Leipzig, Linnestrasse 5, D-04103 Leipzig, Germany

(Received 10 March 2006; revised manuscript received 25 May 2006; published 17 July 2006)

High-quality single crystals of ZnO in the as-grown and N⁺ ion-implanted states have been investigated using a combination of three experimental techniques—namely, positron lifetime/slow positron implantation spectroscopy accompanied by theoretical calculations of the positron lifetime for selected defects, temperature-dependent Hall (TDH) measurements, and deep level transient spectroscopy (DLTS). The positron lifetime in bulk ZnO is measured to be (151 ± 2) ps and that for positrons trapped in defects (257 ± 2) ps. On the basis of theoretical calculations the latter is attributed to Zn+O divacancies, existing in the sample in neutral charge state, and not to the Zn vacancy proposed in previous experimental work. Their concentration is estimated to be 3.7×10^{17} cm⁻³. From TDH measurements the existence of negatively charged intrinsic defects acting as compensating acceptors is concluded which are invisible to positrons—maybe interstitial oxygen. This view is supported from TDH results in combination with DLTS which revealed the creation of the defect $E1$, and an increase in concentration of the defect $E3$ after N⁺ ion implantation, and peculiarities in the observation of the defect $E4$.

I. INTRODUCTION

Zinc oxide (ZnO), a wide band gap (~ 3.4 eV at 300 K) semiconductor material, is presently receiving worldwide attention because of fundamental advantages over GaN in the quest for blue/UV light emitters and detectors, as well as high-speed, high-power, high-temperature, and high-irradiation environment electronic devices.[1,2] Several potential applications require the preparation of ZnO as a thin film or nanowire on monocrystalline substrates such as ZnO, GaN, Si, or sapphire. Although nominally undoped ZnO is already n-type conducting and its resistivity can be decreased down to about 10^{-4} Ω cm by doping with Ga or Al,[2,3] reproducible p doping is still an unsolved problem. The existence and role of native point defects regarding conductivity type and other properties of ZnO has been extensively discussed from a theoretical point of view.[4–6] Engineering of the optical band gap of ZnO has been demonstrated, i.e., by shifting to higher or lower values by alloying with MgO (Refs. 7–9) or CdO (Refs. 10 and 11), respectively. It is certain that all types of applications rely on a full understanding of the role of lattice defects, which largely control the optical and electrical properties of semiconductors, and provision of high-quality bulk material and films. Both needs are not yet achieved, but there is rapid development in these fields.

Positron annihilation spectroscopy (PAS),[12,13] especially in the form of slow positron implantation spectroscopy (SPIS) using monoenergetic positrons,[14] is now a well-established tool for the study of electronic and defect properties of bulk solids and thin films. Early studies[15] of nominally pure ZnO single crystals revealed a positron lifetime of (169 ± 2) ps, interpreted as the bulk positron lifetime τ_b, and a longer lifetime of (203 ± 3) ps characterizing "some vacancy-type defect."

A few other early PAS studies of ZnO bulk materials have already been published and are cited and discussed in connection with systematic studies of electron and proton irradiation of nominally pure ZnO followed by isochronal annealing.[16,17] As expected, due to the variety of possible defects in compound semiconductors, and further complicated by the fact that native defects may exist on both sublattices and in different charge states, the interpretation of experimental results is not trivial. These investigations may be summarized as follows: τ_b varies with sample origin, pointing to the influence of grown-in defects which depend on the method of growth. After electron or proton irradiation, three distinct annealing stages were observed[18] at about 200, 500, and 750 °C, in agreement with other studies. After annealing at 1150 °C all radiation-induced defects are found to be annealed out. It was concluded later that the annealing stage at 500–550 °C is most probably connected to the negatively charged Zn vacancy.[19]

Another study[20] of as-grown and electron irradiated ZnO revealed a longer lifetime at low temperatures of

(265 ± 25) ps in the as-grown and of (230 ± 10) ps in the electron-irradiated sample. Within uncertainties both long lifetimes were interpreted to be characteristic of the same open volume defect, i.e., the doubly negatively charged zinc vacancy. Further studies[21,22] of electron irradiation and subsequent annealing of ZnO are based on the previous interpretation[20] of results, in particular having a bulk lifetime of 170 ps at 300 K.

A recent SPIS study[23] of bulk and epitaxial ZnO shows the influence of deposition temperature (570, 630, 800 °C) on both the ZnO film and the substrate, although the authors do not pay attention to the latter fact when discussing their results. Observed changes in ZnO film properties are argued to be connected with the neutral or negatively charged Zn vacancy. This discussion is, however, inconsistent with earlier results that show annealing of this defect at about 500 °C (Refs. 16–18), and no reference is made to the annealing step at about 750 °C (Refs. 16–18) visible in the experimental data.[23]

Another recent SPIS study deals with the characterization of undoped ZnO single crystals, implanted with Al$^+$ ions at various fluences and then annealed at various temperatures up to 900 °C, by positron lifetime and Doppler broadening measurements.[24] Interestingly, results of a rather pragmatic positron lifetime calculation are presented. A bulk lifetime of $\tau_b \sim 158$ ps is found, and the lifetime representing positron annihilation at the Zn vacancy is given as ~ 188 ps. In addition, the lifetime representing positron annihilation at the Zn+O divacancy and multiples of it are considered.

In theoretical calculations[25] of positron lifetimes in MgO and ZnO two different approaches to electron-positron correlations have been used. In the case of ZnO this results in values of 144 and 153 ps for the bulk lifetime and 200 and 217 ps for the Zn vacancy lifetime. In addition, experimental values of 153 ps (bulk) and 202 ps (Zn vacancy) are reported for specimens prepared by sintering ultrahigh purity ZnO powder. To our knowledge, no theoretical calculations of the positron-related defect properties of ZnO which would include lattice relaxations around defects have been published.

Another work[26] performed recently on differently sintered polycrystalline ZnO powders reports three positron lifetime components, attributing the shortest ($\tau_1 \sim 145$ ps) to the free annihilation of positrons. The intermediate component τ_2 (~ 300–340 ps) is attributed to defect sites representing the clustering of Zn vacancies, and the low-intensity long component τ_3 (1–2 ns) to pick-off annihilation from ortho-positronium which may form in the large open volume among grains.

Temperature-dependent Hall effect (TDH) measurements and deep level transient spectroscopy (DLTS) yield information about dominant donors (thermal activation energy, density) and scattering mechanisms (density of compensating acceptors), or about the thermal activation energy, concentration, and capture cross-section of energetically deep defects in the band gap, respectively.

Comprehensive studies of the electrical properties of ZnO single crystals grown by seeded chemical vapor transport, by pressurized melt growth, the hydrothermal method, and ZnO thin films grown by pulsed laser deposition on sapphire substrates can be found, e.g., in Refs. 27–29. The dominant donors have thermal activation energies in the wide range between about 20 and about 370 meV, though the latter are only found in highly compensated samples grown by the hydrothermal method. Defect levels with thermal activation energies of about 35, 51, and about 65 meV have tentatively been attributed to interstitial hydrogen (H$_i$), or interstitial zinc atoms (Zn$_i$), or effective mass donors like Al atoms replacing Zn (Al$_{Zn}$).

The effect of thermal treatment in different atmospheres on the electrical properties shows[1,30,31] that the shallow donor (H$_i$) can be driven out of the crystal during annealing.[1,32] If the annealing is carried out in a deuterium atmosphere it is found that acceptors are compensated by the introduction of a shallow donor state with a thermal activation energy of about 36 meV.[30] Furthermore, annealing in vacuum at about 650 K may cause the formation of a degenerate layer at the surface of ZnO that hinders the accurate determination of the electrical properties of the bulk.[31]

Deep levels that have been observed in state-of-the-art substrate material are the defects $E1$, $E2$, $E3$, and $E4$ having thermal activation energies of about 120, 100, 300, or 540 meV, respectively.[27–29,33] The few reports concerning the introduction of deep electron traps in ZnO by proton implantation or α-particle irradiation commonly show the formation of a defect with similar thermal activation energy as $E4$ (Refs. 34–36) and another deeper defect lying about 0.9 eV below the conduction band.[35,36] Using optical DLTS the creation of a hole trap is observed,[36] lying about 160 meV above the valence band maximum by proton implantation.

In the present work, three different techniques—PAS/SPIS, TDH, and DLTS—are employed to characterize ZnO single crystals and their defect states. These three techniques study materials from different viewpoints but, as demonstrated here, when their results are taken together the credibility and reliability of interpretations arrived at are substantially increased compared to the case when just one technique is used.

We summarize briefly important features of the three techniques in relation to defect studies. There are three aspects to be considered. First, defects connected with a free volume (vacancies and related defects) can be detected using PAS, in principle. Second, as for the position of the defect-related energy level in the band gap of an n-type material, the TDH method can be used to examine shallow donors (i.e., donors having their corresponding levels close to the conduction band edge) and all compensating acceptors. The DLTS technique then enables us to study defects with corresponding levels positioned deep in the band gap. The third aspect is the charge state of defects. Neutral or negatively charged defects are attractive for positrons while both the TDH and DLTS techniques generally detect charged defects only. Finally, it should be mentioned that there is no obvious relation between the free volume of a defect and the position of the corresponding energy level or the defect charge state. This complicates making direct correlation between the results of PAS measurements and the other two techniques employed.

The paper is organized as follows. In Sec. II experimental details are given, Sec. III briefly describes methods used for

structural relaxations and positron calculations for selected defects, and in Sec. IV the experimental and theoretical results are presented and discussed. Conclusions are drawn in Sec. V.

II. EXPERIMENTAL

Two high quality ZnO single crystals of dimensions $10 \times 10 \times 0.3$ mm^3, grown using a pressurized melt growth approach, were supplied by Cermet, Inc. (Atlanta/GA). Each crystal had the Zn-face lapped and the O-face polished. For the purpose of comparison, one crystal was given an additional refined chemical-mechanical polishing on both faces.[37]

Conventional positron lifetime spectroscopy (PLS) was performed at Rossendorf with a time resolution (full width at half maximum) of about 250 ps and accumulation of about 10^6 total counts in the spectrum.

SPIS measurements were carried out with the monoenergetic positron beam[38] "SPONSOR" at Rossendorf at which a variation of the positron energy E from 30 eV to 36 keV with a smallest step width of 50 eV, if required, is possible. The energy resolution of the Ge detector at 511 keV is (1.09 ± 0.01) keV, resulting in a high sensitivity to changes in material properties from surface to depth. About 10^6 events per spectrum were accumulated.

The motion of the electron-positron pair prior to annihilation causes Doppler broadening of the 511 keV annihilation line and can be characterized by the line shape parameters S and W. The usefulness of these parameters may be illustrated further by an S-W plot, which allows one to conclude whether the changes are due to a change in concentration or type of a defect. For a more general discussion of these parameters we refer to the literature.[12,13] In brief, the value of S is defined by the ratio of counts in the central region of the annihilation gamma peak to the total number of counts in the peak. It is common to define the central region for a certain sample to obtain $S \sim 0.5$ for the ZnO reference sample. The value of W is defined as the ratio of counts in the high-momentum regions symmetrical to the peak and the total number of counts so that $W \sim 0.03$ for the ZnO reference sample. The same regions are then used to calculate the values of S and W for every other sample studied. The depth information was obtained from the correlation of S and W with positron energy E using the versatile program package VEPFIT (Ref. 39), in which a density of 5.605 g/cm^3 for ZnO was used.

After the PLS and SPIS measurements were finished, the polished side (O face) of the as-received ZnO single crystal was implanted at Rossendorf with N$^+$ ions of 150 keV to a fluence of 10^{14} cm^{-2} perpendicular to the sample surface at a substrate temperature of 300 °C.

TDH measurements were performed in the temperature range 20–325 K at Leipzig using an automated Hall setup (Keithley 220 programmable current source, Keithley 7001 switch equipped with a 7065 Hall card, Keithley multimeter 2000, a Lakeshore 330 temperature controller, HP 6030 A as power supply for the magnetic coils). Annealing in air for 30 min of both the un-implanted and ion-implanted samples was performed at 500 °C.

DLTS measurements were performed in the temperature range 20–300 K at Leipzig using a PhysTech FT1030 DLTS System. The existence of a space charge region, for example in a Schottky diode, is a necessity for DLTS measurements. Pd contacts on the top surfaces of the two samples were realized by thermal evaporation. Ohmic contacts were realized on the back side by sputtering Au with a power of 60 W. The Schottky diodes exhibited good rectifying behavior as was controlled and confirmed by current-voltage measurements.

III. COMPUTATIONAL METHODS

In order to elucidate the nature of observed positron trapping sites in ZnO and to support directly the interpretation of experimental positron data, we performed the structural relaxation of several types of vacancylike defects in ZnO and calculated positron characteristics for them. In particular, the Vienna *ab initio* simulation package[40] (VASP, version 4.6.21) using local density approximation (LDA) ultrasoft pseudopontials[41] supplied along with the package was employed to obtain relaxed defect geometries. Then, positron calculations were carried out by means of the atomic superposition (ATSUP) method[42] thereby using relaxed defect configurations. In positron calculations the approaches to electron-positron correlations of Boroński-Nieminen[43] (BN) (with the correction[44] for incomplete positron screening with the high frequency dielectric constant $\epsilon_\infty = 4$) and of Barbiellini *et al.*[45]—a gradient correction (GC) scheme—are used.

ZnO exhibits the hexagonal wurtzite structure (space group $P6_3mc$, group number 186) and the lattice parameters ($a = 0.32501$ nm and $c = 0.52071$ nm) were taken from Ref. 46. In addition to bulk ZnO the vacancy-type (indication: V) V_O, V_{Zn} and (nearest neighbor) V_{Zn+O} defects have been examined, the last being considered in two nonequivalent configurations [labeled $V_{Zn+O}(1)$ and $V_{Zn+O}(2)$]. For VASP calculations, supercells containing 48 ZnO "molecules" (96 atoms) were employed using the Brillouin zone sampling with eight **k**-points (Γ centered **k** mesh with division $2 \times 2 \times 2$). The starting defect configurations for studied vacancy-like defects were obtained by removing appropriate atoms from the ZnO lattice. The total energy of cells was then relaxed with respect to atomic positions. In all calculations, the charge state of defects is supposed to be neutral. The calculated band gap of ZnO amounts to 1.9 eV (see Ref. 4) and is apparently smaller than its experimental counterpart (3.4 eV) that can be ascribed to the well-known LDA band gap error. The detailed results of electronic structure calculations and structure relaxations will be published elsewhere.[47]

For the purpose of positron calculations, the relaxed VASP supercells were extended to a total of 180 "molecules" (360 atoms) by adding atoms at sides of VASP supercells. Such added atoms are arranged in the form of the regular ZnO lattice. The effect of positron-induced relaxations is neglected in this work. The positron lifetimes for bulk ZnO and studied defects were calculated[48] using corresponding ground state positron wave functions and considering the abovementioned approaches to electron-positron correla-

TABLE I. Results of positron calculations (see the text for the corresponding description of abbreviations used). Symbols τ and E_b stand for the positron lifetime and positron binding energy to defects, respectively (lifetimes and binding energies for nonrelaxed configurations are specified in parentheses). Lattice relaxations (related to the lattice constant a) due to the removal of a zinc and/or oxygen atom from the lattice are also given (second column). Here the first number corresponds to the average relaxation of Zn first nearest neighbors of defects; the second number applies to O first nearest neighbors. The "+" or "−" signs indicate that the relaxation is inward or outward with respect to a defect, respectively.

Defect	Relaxation (%)	ATSUP-BN		ATSUP-GC	
		τ (ps)	E_b (eV)	τ (ps)	E_b (eV)
bulk	—, —	159		176	
V_O	+4.6, —	159 (160)	0.01 (0.02)	177 (178)	0.01 (0.02)
V_{Zn}	—, −9.7	229 (194)	0.60 (0.35)	257 (211)	0.50 (0.22)
$V_{Zn+O}(1)$	−17.1, −11.4	286 (224)	1.23 (0.61)	327 (250)	1.19 (0.54)
$V_{Zn+O}(2)$	−14.6, −7.5	276 (223)	1.10 (0.61)	313 (250)	1.06 (0.54)

tions. The positron binding energy to a defect was obtained as a difference of the ground state positron energies for bulk and the corresponding defect. Finally, the bulk lifetime calculations were checked using the linear-muffin-tin-orbital (LMTO) method.[49]

IV. RESULTS AND DISCUSSION

A. Theoretical calculations of positrons states

First, we discuss bulk lifetimes. Table I gives calculated ATSUP values. Bulk lifetimes calculated using the LMTO method amount to 153 and 171 ps using the BN and GC computational schemes, respectively. In both cases lifetimes are slightly shorter than their ATSUP counterparts, but still the agreement between the ATSUP and LMTO methods appears to be reasonable. This warrants using the ATSUP method in further calculations, though it is a non-self-consistent method with respect to electronic degrees of freedom.

The results of ATSUP positron calculations both for relaxed and nonrelaxed defect configurations are summarized in Table I. As for lattice relaxations, except for the V_O defect and the bulk, their effect is found to be quite large. Therefore, a pair of numbers in Table I is given that characterizes the amount of relaxation of defect first nearest neighbors.

It is obvious that the oxygen vacancy does not represent a positron trap as its binding energy is negligible regardless of whether relaxations effects are included or not; the inward relaxation of nearest neighbor Zn atoms further decreases the free volume corresponding to the defect. In the case of other defects where a Zn vacancy is involved, the relaxations are large and predominantly of outward character, which results in longer positron lifetimes compared to the nonrelaxed case. This effect is related to rebonding of oxygen atoms around defects and will be discussed in detail in a separate publication[47] and compared with existing literature (see, e.g., Refs. 5 and 6). The lifetime results are further discussed in terms of experimental positron data in the next subsection.

Finally, we note that in Ref. 25 a somewhat longer lifetime was calculated within the BN scheme for the unrelaxed Zn vacancy. Partly, this is due to a different dielectric con-

stant ϵ_∞ used in Ref. 25 and, partly, the reason is unknown. On the other hand, our BN values for the Zn vacancy and Zn+O divacancy agree well with those obtained in Ref. 24.

B. Positron studies of virgin samples

Positron lifetimes in ZnO reported in earlier investigations[16,17] may be summarized as follows: τ_b =185 ps for sintered polycrystalline ZnO (1200 °C/18 h): τ_b=183 ps for an as-received single crystal (origin not given), which decreases slightly to τ_b=180 ps after further annealing [1150 °C/2 h, slow cooling (100 h) to room temperature]: τ_b=176 ps for another single crystal (CrysTec, Berlin): and much shorter values of τ_b=(158−162) ps for other ZnO single crystals (Eagle-Picher, Miami/FL), either as-received or annealed as above. Positron lifetimes connected with open volume defects are given and interpreted as τ_d=(209±6) ps for the negatively charged Zn vacancy, τ_d=(260±7) ps for the negatively charged Zn divacancy, and τ_d=(370±20) ps for "a larger defect agglomerate which forms during post-irradiation annealing."

Tuomisto *et al.*[20] demonstrated that the defect having a lifetime of (230±10) to (265±25) ps was negatively charged using temperature-dependent lifetime measurements, but identified it as the doubly negatively charged Zn vacancy.[20] The same authors interpreted a positron lifetime of 170 ps as the bulk lifetime.

In our as-received bulk samples, free fitting shows the existence of a two component spectrum with the following positron lifetimes and intensities τ_1=(93±3) ps, τ_2=(257±2) ps, I_1=(39.9±0.7) %, and I_2=(60.1±0.7) %. The agreement of τ_2 with the value τ_d=(260±7) ps, previously associated[16,17] with the negatively charged Zn divacancy, is remarkable. From the estimated intensities it is certain that no saturation trapping of positrons in our crystals exists, and hence the simultaneous presence of negatively charged Zn vacancies, supposed to be characterized by τ_d=(209±6) ps (Refs. 16 and 17), may be excluded. The application of the one-state trapping model[12,13] gives a bulk lifetime of τ_b=(151±2) ps. This value is in remarkable agreement with experimental values given in Refs. 25 and 26, and therefore

it is confidently considered to represent defect-free bulk ZnO. As this lifetime is shorter than those reported for as-grown samples of other origin,[16,17,20] it has to be concluded that samples investigated previously must have contained grown-in defects of yet unknown configuration which are able to trap a positron.

From the various bulk and defect positron states in ZnO that have been considered by different theoretical approaches (Table I) it becomes obvious that here the BN approach seems to fit best the experimental situation known so far from the literature, and including the present results. Though usually the GC approach gives bulk lifetimes that are very close to experimentally observed ones, in the case of ZnO the situation is different and a further study is needed to clarify this point.

Within the BN scheme of calculations, a short bulk value of 159 ps and two longer defect state lifetimes, i.e., of the Zn vacancy and the Zn+O divacancy, are well described regardless of the fact that the lattice relaxation might not be described perfectly due to the neglect of positron induced relaxations—compare the corresponding experimental values of $\tau_d=(209\pm6)$ ps and $\tau_d=(260\pm7)$ ps, taken from Refs. [16] and [17]. The fact that our calculations consider neutral defects only should be of negligible impact (see Ref. [48] for related discussion). Therefore, taking the experimental facts[16,17,20] together with our theoretical results one associates the lifetime $\tau_d=(260\pm7)$ ps with the negatively charged Zn+O divacancy. In our opinion, this interpretation is to be favored against the negatively charged Zn divacancy[16,17] because for structural reasons, similar to the case of 6H-SiC,[50] the positron should consider this defect almost like a single vacancy despite its charge. On the other hand, the adjustment[51] of the calculation scheme to give lifetimes for the bulk and Zn vacancy of 177 and 237 ps, respectively (Ref. [20]), is unproductive because it totally ignores the previously observed defect characterized by a lifetime of $\tau_d=(209\pm6)$ ps (Refs. [16] and [17]).

The trapping rate κ is proportional to the defect concentration. The proportionality constant is the so-called trapping coefficient (ν).[13] Trapping coefficients for monovacancies and divacancies of different charge states in semiconductors were reviewed recently in Ref. [13]. For the sake of defect concentration estimates, we employ here average values from Ref. [13] as direct information about trapping coefficients for defects in ZnO is not available at present. Considering then that a negatively charged Zn+O divacancy has the trapping coefficient $\nu=5\times10^{15}$ s⁻¹ and taking $\kappa=4.12$ ns⁻¹, as determined from our positron lifetime measurements, it is possible to deduce the concentration of negatively charged Zn+O divacancies to be about 8.0×10^{-7} per atom in our samples. From our room temperature experiments we may strictly only connect the Zn+O divacancy with $\tau_2=(257\pm2)$ ps but not identify its charge state, i.e., whether it is neutral or negatively charged. However, in the case of being electrically neutral its atomic concentration should be about 4.6×10^{-6} [using $\nu=9\times10^{14}$ s⁻¹ (Ref. [13])] for the same trapping rate $(\kappa=4.12$ ns⁻¹).

The relation between the atomic (C_{at}) and volume (C_{vol}) concentrations is given by $C_{vol}=C_{at}/\Omega$, where Ω is the vol-
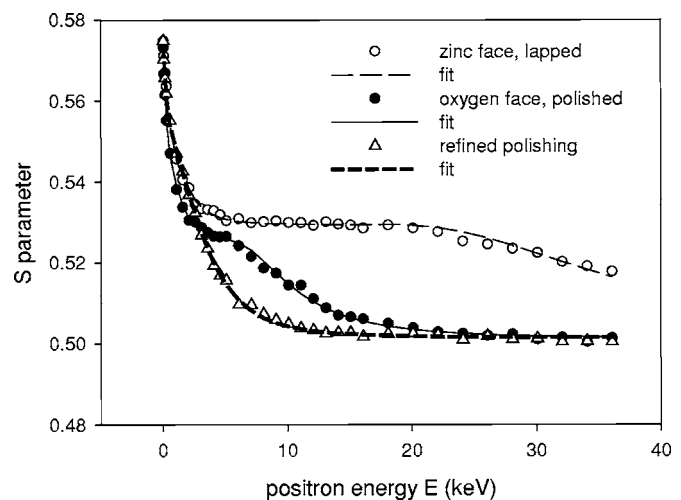

FIG. 1. Doppler broadening parameter S of a virgin ZnO single crystal as a function of incident positron energy E in as-received state (lapped, polished) and with improved surface quality (refined polishing). The best fit to the data is shown.

ume per atom. According to the lattice parameters[46] used in calculations (see Sec. III), we obtain a value of $\Omega=11.91\times10^{-24}$ cm³. This yields volume concentrations $C_{vol}=6.7\times10^{16}$ and 3.7×10^{17} cm⁻³ for the negative and neutral divacancies, respectively. We consider these numbers as an order of magnitude estimates because the precise values of trapping coefficients for vacancy-like defects in ZnO are not known.

SPIS results for the as-received virgin ZnO sample are shown in Fig. 1. It is obvious that there is a damaged subsurface layer introduced by lapping (zinc face) and polishing (oxygen face), estimated by VEPFIT analysis[39] to extend as deep as $d=(1942\pm32)$ nm and $d=(231\pm5)$ nm, respectively. The result of giving the as-received sample an additional refined polishing on both faces is a removal of these damaged layers—as can be seen from the SPIS results presented in Fig. 1. The improved surface quality becomes obvious from the fact that measured data points obtained on both faces now almost coincide. Fitting the data measured at the improved Zn face results in a positron diffusion length $L_+=(50\pm1)$ nm which is quite reasonable compared to a value of 52 nm reported recently[23,52] for a ZnO single crystal of different origin (Eagle-Picher, Miami/FL), and with a value of (50 ± 5) nm reported also recently for ZnO films grown by metal-organic chemical vapor deposition on sapphire.[53]

C. SPIS studies of the N⁺ ion-implanted sample

To illustrate the extent of the subsurface region damaged by ion implantation the profiles of ions and vacancies due to the implantation estimated by TRIM calculations[54] are shown in Fig. 2. It is clear that the vacancy distribution differs from that for ions; the maxima are at depths of ~200 and ~270 nm, respectively.

In Fig. 3 SPIS results are presented. By VEPFIT analysis[39] it is estimated that a damaged layer is created by the ion implantation that extends to $d=(354\pm7)$ nm.
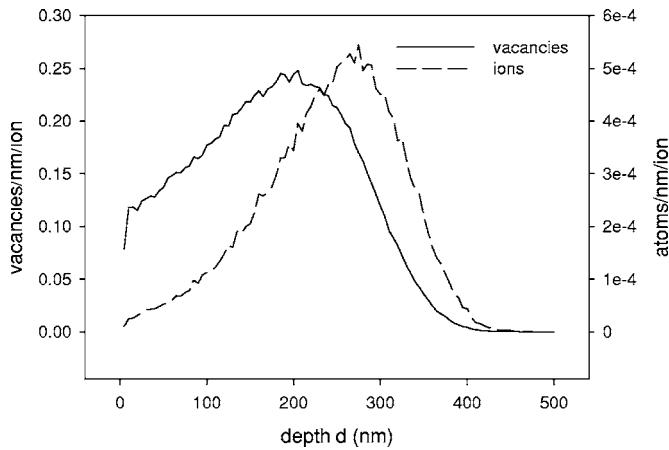
FIG. 2. Ion and vacancy distribution in ZnO films calculated by TRIM (Ref. 54).

When only two distinct annihilation characteristics, described by (S_1, W_1) and (S_2, W_2), contribute to a set of experimental data, a straight line is obtained in the S-W representation where the endpoints represent the two states. Although we do not yet know the (S, W) coordinates representing a perfect ZnO bulk, it is useful to display all our measured data in one plot—see Fig. 4. It shows that the same type of damage, as created from polishing and lapping by the supplier of the crystals, is created by ion implantation, i.e., open volume damage.

After N^+ ion implantation the sample was annealed at 500 °C in air for 30 min. Figure 3 shows a comparison of the $S(E)$ curves of the as-implanted sample and the same sample after annealing. No remarkable difference is visible, suggesting that the annealing at 500 °C did not influence the vacancy-type defects created by the surface treatment of the sample and by the N^+ ion implantation.
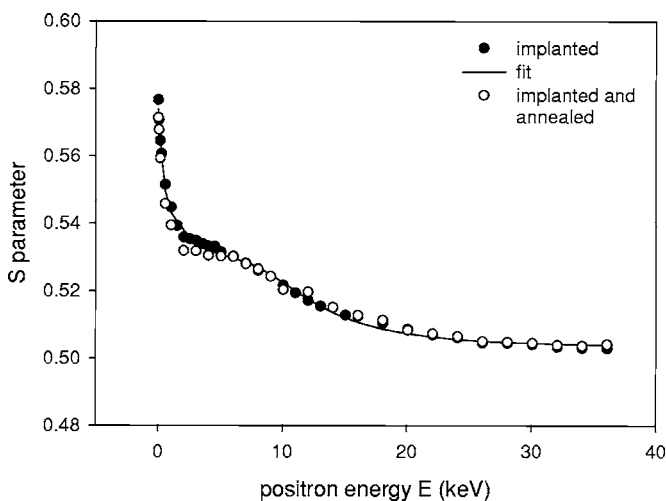

FIG. 3. Doppler broadening parameter S of a ZnO single crystal implanted with N^+ ions of 150 keV to a fluence of 1×10^{14} cm^{-2} at 300 °C and after thermal annealing at 500 °C as a function of incident positron energy E. The best fit to the as-implanted data is shown.
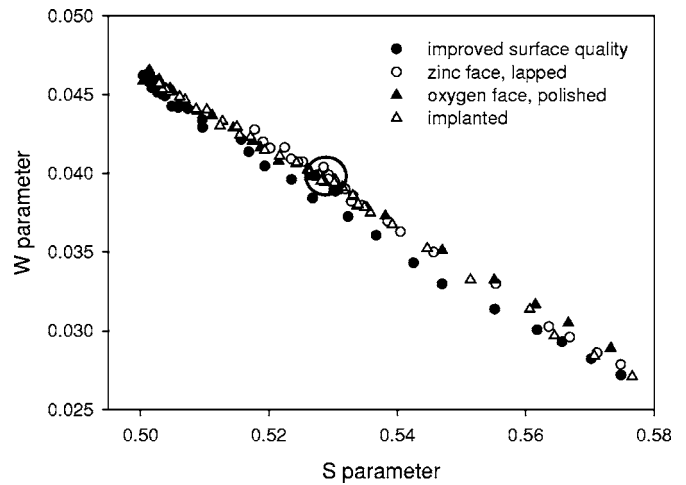

FIG. 4. *S-W* plot of various SPIS data measured on ZnO crystals of different treatments.

D. TDH measurements

TDH measurements were performed on the as-grown and the N^+ ion-implanted sample. While Hall experiments represent an integral measurement over the whole sample thickness, and therefore, in principle, are not suited for samples having gradients in their impurity distribution, the data obtained for the N^+ ion-implanted sample are nevertheless considered useful for a first qualitative comparison.

Hall mobility data of the as-grown and the N^+ ion-implanted sample as a function of temperature are depicted in Fig. 5. Peak Hall mobilities of 1470 cm^2/V s (at 60 K) and 1310 cm^2/V s (at 63 K) are observed for the nonimplanted or the ion-implanted sample, respectively, suggesting a higher density of negatively charged defects in the N^+ ion-implanted sample. The corresponding fits consider ionized impurity, acoustic deformation and a piezoelectric potential, as well as polar optical scattering. The Hall scattering factor used for the analysis is set to unity, and the total mobility was calculated using Matthiessen's rule. Although the N^+ ion implantation depth is much smaller than the sample thickness, the influence of the implantation on the Hall mobility is clearly visible.
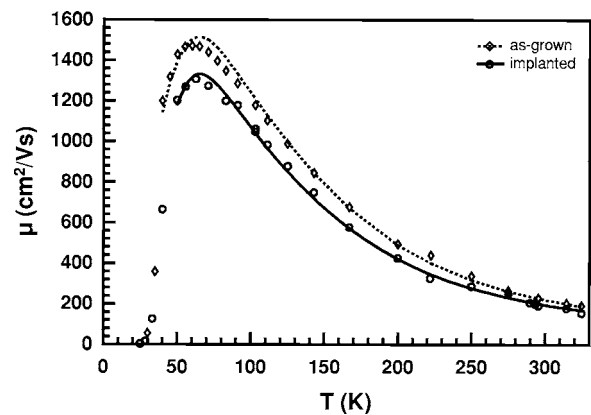

FIG. 5. Hall mobility (markers) and corresponding fit (lines) for as-grown and ion-implanted ZnO.
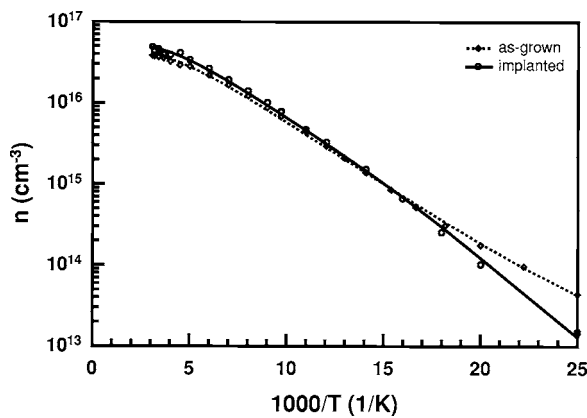
FIG. 6. Free electron concentration (markers) and corresponding fits (lines) for as-grown and ion-implanted ZnO.
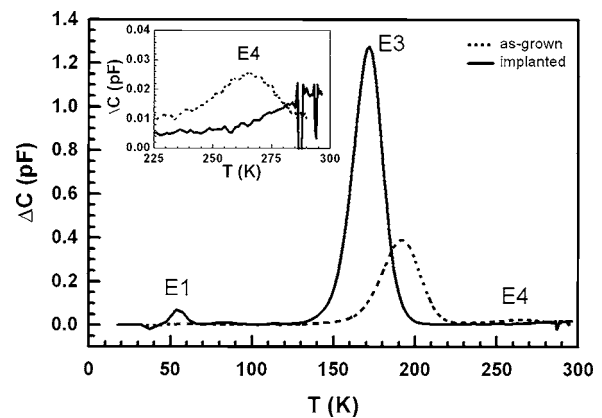

FIG. 7. DLTS signal of as-grown (rate window 200 Hz) and ion-implanted (rate window 10 Hz) ZnO. The inset depicts the high temperature data with different y scales.

The acceptor densities obtained from the fits—calculated for the entire sample thickness—equal to 3.9×10^{15} and 4.5×10^{15} cm^{-3} for the unimplanted and the implanted sample (assuming singly negatively charged acceptor states). Again, these densities cannot be compared quantitatively, but confirm the presence of a significantly higher acceptor density due to N⁺ ion implantation, possibly indicating the incorporation of nitrogen atoms on oxygen lattice positions.

Generally, a multilayer model[55] might be applied to separate the contributions of the bulk and the small part of the sample affected by the N⁺ ion implantation. However, this implies that the electrical properties of the bulk part of the as-grown and the N⁺ ion-implanted sample are identical—which is not the case here. Therefore, in future the same sample should be measured before and after N⁺ ion implantation.

The free electron concentration n of the as-grown and the N⁺ ion-implanted sample is depicted in Fig. 6 as a function of reciprocal temperature. The corresponding fits are obtained by solving the two-donor charge balance equation using the acceptor densities determined from the fit of the Hall mobility. The best fits yield a thermal activation energy of the dominant donor of (50.8 ± 0.5) meV for both kinds of samples. The density is $(4.8 \pm 0.2) \times 10^{16}$ cm^{-3} and $(6.3 \pm 0.3) \times 10^{16}$ cm^{-3} for the nonimplanted and N⁺ ion-implanted sample, respectively.

The thermal ionization of this donor dominates the temperature dependence of n for $T > 70$ K. The chemical origin of this defect is still under debate to date. Hutson[56] proposed interstitial zinc atoms Zn_i to cause this level. However, our experiments provide evidence that interstitial zinc has lower thermal activation energy and thus the chemical origin of this donor cannot be clarified within the framework of experiments presented here. For temperatures lower than 70 K shallow donors with densities of about $(4 \pm 0.8) \times 10^{15}$ or $(5 \pm 0.9) \times 10^{15}$ cm^{-3} and activation energies of (16.1 ± 3) or (22 ± 3) meV are observed for the nonimplanted or the N⁺ ion-implanted sample, respectively.

The density of negatively charged acceptors of the virgin sample determined from the analysis of the Hall mobility is about an order of magnitude lower than the calculated density of Zn+O divacancies determined from positron lifetime studies (Sec. IV B). Therefore the upper limit of the concentration of the negatively charged Zn+O divacancy is the density of compensating acceptors of 3.9×10^{15} cm^{-3} determined from the fit of the Hall mobility. Quite formally, the lower limit of the density of neutral Zn+O divacancies in the nonimplanted sample can be calculated to be $(6.7 \times 10^{16} - 3.9 \times 10^{15}$ cm$^{-3}) \simeq 6.3 \times 10^{16}$ cm^{-3}. However, in n-type ZnO, where the Fermi level is close to the conduction band, all acceptors should be negatively charged. To explain this discrepancy maybe due to an unknown value of trapping coefficient for vacancylike defects in ZnO is also unlikely, similar to assuming maybe a doubly negatively charged Zn vacancy. Therefore, it has to be questioned at all if the Zn+O divacancy is really acting as an acceptor. This implies these divacancies to be neutral, and thus their concentration is 3.7×10^{17} cm^{-3}—as already estimated above. The solution of the apparent dilemma could be the existence of a negatively charged intrinsic defect acting as main acceptor which is invisible to positrons—this could be interstitial oxygen.[57,58] However, it is also known that the Zn source used for the pressurized melt growth may contain group I elements that would also introduce acceptor states if incorporated at Zn sites.

Nevertheless it is an experimental fact that the density of open volume defects increases due to N⁺ ion implantation, as the positron studies reveal (see Fig. 4). Additionally, the density of negatively charged defects (acceptors) increases due to N⁺ ion implantation too, as confirmed by the TDH measurements. Current wisdom connects ion implantation into a crystalline material with simultaneous formation of vacancy-type and interstitial defects.[54] Thus, the formation of vacancies and interstitials of zinc and oxygen have to be assumed. Combinations of such simple defects might also form, but from present TDH and positron results alone it cannot be decided which defects finally are acting as acceptors.

E. DLTS measurements

DLTS signals of the two diodes investigated are depicted in Fig. 7 (for different rate windows, to aid clarity). The as-grown sample shows two peaks that can be related to the

defects $E3$ (trap density $N_t \sim 3.2 \times 10^{15}$ cm^{-3}) and $E4$ ($N_t \sim 2.6 \times 10^{14}$ cm^{-3}), which have commonly been observed[27,33,59,60] in ZnO. These electron traps have thermal activation energies E_t of 310 or 530 meV, respectively. From Fig. 7 it is obvious that the N^+ ion-implanted sample contains an additional trap labeled $E1$ with $E_t \sim 120$ meV and $N_t \sim 6.6 \times 10^{14}$ cm^{-3}. This defect has been suggested[22] to be possibly related to V_O, but additional experimental evidence has been requested at the same time to clarify the identity of $E1$.

From TDH results discussed above it has been suggested that the main acceptor could be the oxygen interstitial—with an increase in concentration of $(4.5-3.9) \times 10^{15}$ cm^{-3} = 6 $\times 10^{14}$ cm^{-3} due to ion implantation. This value almost equals the density of $E1$ observed after implantation and thus supports the interpretation of being connected with the defect V_O. We like to note, that due to the inhomogeneous defect depth distribution in the ion-implanted sample, one would expect that the density of the $E1$ defect determined by DLTS is larger than the increase of the density of compensating acceptors determined from the integral Hall measurement. However, the increase in concentration of compensating acceptors is—within experimental error—equal to the concentration of the $E1$ defect created during implantation. This can be explained by the fact that both sublattices are affected by N^+ ion implantation and the increase in the density of compensating acceptors (determined by TDH) reflects both the creation of acceptorlike Zn vacancies and acceptorlike oxygen interstitials.

Furthermore, the concentration of $E3$ is, at 8.8 $\times 10^{15}$ cm^{-3}, almost a factor of 3 larger than for the unimplanted sample. Most probably $E3$ is also connected to an intrinsic defect, maybe the second ionization level of Zn_i. The observed increase of 5.6×10^{15} cm^{-3} is about one order of magnitude larger than in case of V_O or the oxygen interstitial. This fact may be compared to electron irradiation experiments[18] where an oxygen displacement rate about one order-of-magnitude less than the zinc displacement rate has been found. If $E3$ is connected with an increase in the concentration of Zn_i, then its counterpart V_{Zn} has to be created as well. Indeed, the SPIS results (see Sec. IV C) indicate the formation of open volume damage due to the ion implantation which is stable against the performed annealing at 500 °C for 30 min. However, depth-dependent positron lifetime measurements would have been necessary to further characterize this damage in the narrow subsurface layer of (354 ± 7) nm, but were not available.

In addition, the comparison of TDH and DLTS results shows that the concentration of the shallow donors matches the concentration of the defect $E3$ for both types of samples very well. We propose now that the shallow donor observed represents the first ionization level of Zn_i and $E3$ represents the second ionization level of Zn_i. Due to the inhomogeneous depth distribution of defects in the ion-implanted sample it is clear that the concentration of $E3$ (as determined by DLTS) must be higher than the concentration of shallow donors (determined from the integral TDH measurement). Early experiments on Zn doped ZnO revealed thermal activation energies between about 11 and 23 meV (depending on the donor density) which are in good agreement with the thermal activa-

tion energies of the shallow donors found in our samples underlining the tentative attribution to be connected to Zn_i (Refs. [61–63]).

Surprisingly, the defect $E4$ was not detectable in the implanted sample due to the superposition of electronlike and holelike transients in the temperature range between about 260 and 310 K. However, a p-conducting layer is formed at the surface of the N^+ implanted sample after thermal treatment performed, that can be used to inject holes into the n-type bulk part of the sample. These results will be presented and discussed in detail elsewhere.[64]

V. CONCLUSIONS

The sensitivity of PAS/SPIS to open-volume defects in ZnO single crystals, already indicated from earlier studies in the literature, is further demonstrated by the present experimental work. A consistent theoretical modeling of bulk and defect positron properties of ZnO using the ATSUP method with and without lattice relaxation is given. This allows one to conclude that an experimental positron lifetime[16,17] of $\tau_d = (260 \pm 7)$ ps, in almost exact agreement with our value of $\tau_2 = (257 \pm 2)$ ps, is most probably connected with positron trapping at the neutral Zn+O divacancy, allowing the estimation of a defect concentration.

The surface quality of ZnO single crystals and their improvement is demonstrated by PAS/SPIS and a measure of the bulk quality is given in terms of various positron parameters. The observation of subsurface open-volume damage present in the "virgin" material should be of special importance to optical and electrical investigations and their interpretation. In addition, the detection of radiation damage created by ion implantation and its annealing is given.

TDH measurements were performed on the as-grown and implanted samples. The Hall mobility has been determined and fitted, considering ionized impurity, acoustic deformation and piezoelectric potential, as well as polar optical scattering. In summary, the dominant donor in pressure melt grown ZnO has a thermal activation energy of about 51 meV. The chemical identity of this defect could not be clarified. Besides this, such samples contain more shallow donors with concentrations in the mid 10^{15} cm^{-3} range which influence the temperature dependence of the free electron concentration for $T < 70$ K. The N^+ ion-implanted sample contains a higher density of the dominant donor. It is concluded that negatively charged intrinsic defects exist which act as compensating acceptors and which are invisible to positrons—most probably interstitial oxygen. This view is supported by the DLTS results.

DLTS measurements performed between about 20 and 300 K showed an increase of the densities of the defect $E3$ and the creation of the defect $E1$ during implantation. With that, we arrive at the following tentative assignments: the shallow donors observed $[E_d \sim (16-22)$ meV, $N_t \sim (4-5) \times 10^{15}$ cm$^{-3}]$ are connected to the first ionization level of Zn_i, and $E3$ $[E_t \sim 310$ meV, $N_t \sim (3-9) \times 10^{15}$ cm$^{-3}]$ to the second ionization level of Zn_i. The dominant acceptor introduced by the implantation process is interstitial oxygen O_i with a concentration of 6×10^{15} cm^{-3}. The defect $E1$ which

is created during the implantation with a concentration of 6.6×10^{14} cm^{-3} is connected to the oxygen vacancy V_O. Peculiarities associated with the observation of the defect $E4$ have led to the detection that N⁺ ion implantation results in the formation of a p-conducting layer close to the surface.

ACKNOWLEDGMENTS

*Electronic address: G.Brauer@fz-rossendorf.de

†Electronic address: Jan.Kuriplach@mff.cuni.cz

‡Electronic address: CMoisson@novasic.com

§Electronic address: Wenckst@physik.uni-leipzig.de

[1] D. C. Look, Mater. Sci. Eng., B **80**, 383 (2001).

[2] *Transparent Conducting Oxides*, edited by D. S. Ginley and C. Bright, Mater. Res. Bull. **25**, 15 (2000).

[3] K. Ellmer, J. Appl. Phys. **34**, 3097 (2001).

[4] C. G. Van de Walle, Phys. Rev. Lett. **85**, 1012 (2000).

[5] A. F. Kohan, G. Ceder, D. Morgan, and Chris G. Van de Walle, Phys. Rev. B **61**, 15019 (2000).

[6] S. B. Zhang, S.-H. Wei, and A. Zunger, Phys. Rev. B **63**, 075205 (2001).

[7] A. Ohtomo, M. Kawasaki, T. Koida, K. Masubuchi, H. Koinuma, Y. Sakurai, Y. Yoshida, T. Yasuda, and Y. Segawa, Appl. Phys. Lett. **72**, 2466 (1998).

[8] C. Bundesmann, M. Schubert, D. Spemann, T. Butz, M. Lorenz, E. M. Kaidashev, and M. Grundmann, Appl. Phys. Lett. **81**, 2376 (2002).

[9] R. Schmidt, B. Rheinländer, M. Schubert, D. Spemann, T. Butz, J. Lenzner, E. M. Kaidashev, M. Lorenz, A. Rahm, H. C. Semmelhack, and M. Grundmann, Appl. Phys. Lett. **82**, 2260 (2003).

[10] T. Makino, Y. Segawa, M. Kawasaki, A. Ohtomo, R. Shiroki, K. Tamura, T. Yasuda, and H. Koinuma, Appl. Phys. Lett. **78**, 1237 (2001).

[11] M. Lorenz, E. M. Kaidashev, H. von Wenckstern, V. Riede, C. Bundesmann, D. Spemann, G. Benndorf, H. Hochmuth, A. Rahm, H.-C. Semmelhack, and M. Grundmann, Solid-State Electron. **47**, 2205 (2003).

[12] *Positron Spectroscopy of Solids*, edited by A. Dupasquier and A. P. Mills, Jr., (IOS, Amsterdam, 1995).

[13] R. Krause-Rehberg and H. S. Leipner, *Positron Annihilation in Semiconductors—Defect Studies* (Springer, Berlin, 1999).

[14] *Slow Positron Beam Techniques for Solids and Surfaces*, edited by G. Brauer and W. Anwand [Appl. Surf. Sci. 194, (2002)] p. 1.

[15] R. M. de la Cruz, R. Pareja, R. González, L. A. Boatner, and Y. Chen, Phys. Rev. B **45**, 6581 (1992).

[16] S. Brunner, W. Puff, P. Mascher, and A. G. Balogh, in *Microstructural Processes in Irradiated Materials*, Mat. Res. Soc. Symp. Proc. No. 540, edited by S. J. Zinkle, G. E. Lucas, R. C. Ewing, and J. S. Williams (Materials Research Society, Warrendale/PA, 1999), p. 207.

[17] S. Brunner, W. Puff, A. G. Balogh, and P. Mascher, Mater. Sci. Forum **363–365**, 141 (2001).

[18] D. C. Look, D. C. Reynolds, J. W. Hemsky, R. L. Jones, and J. R. Sizelove, Appl. Phys. Lett. **75**, 811 (1999).

[19] D. C. Look, R. L. Jones, J. R. Sizelove, N. Y. Garces, N. C. Giles, and L. E. Halliburton, Phys. Status Solidi A **195**, 171 (2003).

[20] F. Tuomisto, V. Ranki, K. Saarinen, and D. C. Look, Phys. Rev. Lett. **91**, 205502 (2003).

[21] F. Tuomisto, K. Saarinen, and D. C. Look, Phys. Status Solidi A **201**, 2219 (2004).

[22] F. Tuomisto, K. Saarinen, D. C. Look, and G. C. Farlow, Phys. Rev. B **72**, 085206 (2005).

[23] T. Koida, S. F. Chichibu, A. Uedono, A. Tsukazaki, M. Kawasaki, T. Sota, Y. Segawa, and H. Koinuma, Appl. Phys. Lett. **82**, 532 (2003).

[24] Z. Q. Chen, M. Maekawa, S. Yamamoto, A. Kawasuso, X. L. Yuan, T. Sekiguchi, R. Suzuki, and T. Ohdaira, Phys. Rev. B **69**, 035210 (2004).

[25] M. Mizuno, H. Araki, and Y. Shirai, Mater. Trans., JIM **45**, 1964 (2004).

[26] S. Dutta, M. Chakrabarti, S. Chattopadhyaay, and D. Jana, J. Appl. Phys. **98**, 053513 (2005).

[27] M. Grundmann, H. von Wenckstern, R. Pickenhain, S. Weinhold, B. Chengnui, and O. Breitenstein, in *Zinc Oxide—A Material for Micro- and Optoelectronic Applications*, Vol. 194 of NATO Science Series II: Mathematics, Physics and Chemistry, edited by N. H. Nickel and E. Terukov (Springer, Berlin, 2005), p. 47.

[28] H. von Wenckstern, S. Weinhold, G. Biehne, R. Pickenhain, H. Schmidt, H. Hochmuth, and M. Grundmann, Adv. Solid State Phys. **45**, 263 (2005).

[29] H. von Wenckstern, M. Brandt, H. Schmidt, G. Biehne, R. Pickenhain, H. Hochmuth, M. Lorenz, and M. Grundmann, Appl. Phys. A (to be published).

[30] C. H. Seager and S. M. Myers, J. Appl. Phys. **94**, 2888 (2004).

[31] O. Schmidt, P. Kiesel, C. G. van de Walle, N. M. Johnson, J. Nause, and G. H. Döhler, Jpn. J. Appl. Phys. **44**, 7271 (2005).

[32] E. V. Monakhov, A. Yu. Kuznetsov, J. S. Christensen, K. Maknys, and B. G. Svensson, Superlattices Microstruct. **38**, 472 (2005).

[33] F. D. Auret, S. A. Goodman, M. J. Legodi, W. E. Meyer, and D. C. Look, Appl. Phys. Lett. **80**, 1340 (2002).

[34] F. D. Auret, S. A. Goodman, M. Hayes, M. J. Legodi, H. A. van Laarhoven, and D. C. Look, Appl. Phys. Lett. **79**, 3074 (2001).

[35] F. D. Auret, L. Wu, W. E. Meyer, J. M. Nel, M. J. Legodi, and M. Hayes, Phys. Status Solidi C **1**, 674 (2004).

[36] A. Y. Polyakov, N. B. Smirnov, A. V. Govorkov, E. A. Kozhukhova, V. I. Vdovin, K. Ip, M. E. Overberg, Y. W. Heo, D. P. Norton, S. J. Pearton, J. M. Zavada, and V. A. Dravin, J. Appl. Phys. **94**, 2895 (2003).

[37] Development of NOVASIC, Le Bourget du Lac/France.

[38] W. Anwand, H.-R. Kissener, and G. Brauer, Acta Phys. Pol. A **88**, 7 (1995).

[39] A. van Veen, H. Schut, J. de Vries, R. A. Hakvoort, and M. R. Ijpma, in *Positron Beams for Solids and Surfaces*, edited by P. J. Schultz, G. R. Massoumi, and P. J. Simpson (American Institute of Physics, New York, 1990), p. 171.

[40] G. Kresse and J. Hafner, Phys. Rev. B **47**, R558 (1993); **49**, 14251 (1994); G. Kresse and J. Furthmüller, Comput. Mater. Sci. **6**, 15 (1996); G. Kresse and J. Furthmüller, Phys. Rev. B **54**, 11169 (1996).

[41] G. Kresse and J. Hafner, J. Phys.: Condens. Matter **6**, 8245 (1994).

[42] M. J. Puska and R. M. Nieminen, J. Phys. F: Met. Phys. **13**, 333 (1983); A. P. Seitsonen, M. J. Puska, and R. M. Nieminen, Phys. Rev. B **51**, 14057 (1995).

[43] E. Boroński and R. M. Nieminen, Phys. Rev. B **34**, 3820 (1986).

[44] M. J. Puska, S. Mäkinen, M. Manninen, and R. M. Nieminen, Phys. Rev. B **39**, 7666 (1989).

[45] B. Barbiellini, M. J. Puska, T. Torsti, and R. M. Nieminen, Phys. Rev. B **51**, R7341 (1995).

[46] E. H. Kisi and M. M. Elcombe, Acta Crystallogr., Sect. C: Cryst. Struct. Commun. **45**, 1867 (1989).

[47] J. Kuriplach *et al.* (unpublished).

[48] M. J. Puska and R. M. Nieminen, Rev. Mod. Phys. **66**, 841 (1994).

[49] For a recent review, see, e.g., O. K. Andersen, O. Jepsen, and M. Šob, in *Electronic Band Structure and its Applications*, edited by M. Yussouff (Springer, Berlin, 1987), p. 1.

[50] G. Brauer, W. Anwand, E.-M. Nicht, J. Kuriplach, M. Šob, N. Wagner, P. G. Coleman, M. J. Puska, and T. Korhonen, Phys. Rev. B **54**, 2512 (1996).

[51] M. Hakala, M. J. Puska, and R. M. Nieminen, Phys. Rev. B **57**, 7621 (1998).

[52] A. Uedono, T. Koida, A. Tsukazaki, M. Kawasaki, Z. Q. Chen, S. F. Chichibu, and H. Koinuma, J. Appl. Phys. **93**, 2481 (2003).

[53] A. Zubiaga, F. Tuomisto, F. Plazaola, K. Saarinen, J. A. Garcia, J. F. Rommeluere, J. Zuniga-Perez, and V. Munoz-Sanjose, Appl. Phys. Lett. **86**, 042103 (2005).

[54] J. F. Ziegler, J. P. Biersack, and U. Littmark, *The Stopping and Range of Ions in Solids* (Pergamon, New York, 1985).

[55] B. Arnaudov, T. Paskova, S. Evtimova, E. Valcheva, M. Heuken, and B. Monemar, Phys. Rev. B **67**, 045314 (2003).

[56] A. R. Hutson, Phys. Rev. **108**, 222 (1957).

[57] S. A. Studenikin, N. Golego, and M. Cocivera, J. Appl. Phys. **84**, 2287 (1998).

[58] H. von Wenckstern, G. Benndorf, S. Heitsch, J. Sann, M. Brandt, H. Schmidt, J. Lenzner, M. Lorenz, A. Yu. Kuznetsov, B. K. Meyer, and M. Grundmann, Appl. Phys. A (to be published).

[59] J. M. Nel, F. D. Auret, L. Wua, M. J. Legodi, W. E. Meyer, and M. Hayes, Sens. Actuators B **100**, 270 (2004).

[60] H. von Wenckstern, S. Heitsch, G. Benndorf, D. Spemann, E. M. Kaidashev, M. Lorenz, and M. Grundmann, in *Physics of Semiconductors: 27th International Conference on the Physics of Semiconductors*, AIP Conf. Proc. No. 772, edited by José Menéndez and Chris G. Van de Walle (AIP, Melville, 2005), p. 183.

[61] P. W. Li and K. I. Hagemark, J. Solid State Chem. **12**, 371 (1975).

[62] B. Utsch and A. Hausmann, Z. Phys. B: Condens. Matter **21**, 27 (1975).

[63] E. Ziegler, A. Heinrich, H. Oppermann, and G. Stöver, Phys. Status Solidi A **66**, 635 (1981).

[64] H. von Wenckstern, R. Pickenhain, H. Schmidt, M. Brandt, G. Biehne, M. Lorenz, M. Grundmann, and G. Brauer, Appl. Phys. Lett. (to be published).